

# Role of tip structure and surface relaxation in atomic resolution dynamic force microscopy: $\text{CaF}_2(111)$ as a reference surface

Adam S. Foster,<sup>1</sup> Clemens Barth,<sup>2</sup> Alexander L. Shluger,<sup>3</sup> Risto M. Nieminen,<sup>1</sup> and Michael Reichling<sup>4</sup>

<sup>1</sup>Laboratory of Physics, Helsinki University of Technology, P.O. Box 1100, 02015 HUT, Finland

<sup>2</sup>CRMC2-CNRS, Campus de Luminy Case 913, 13288 Marseille Cedex 09, France

<sup>3</sup>Department of Physics and Astronomy, University College London, Gower Street, London WC1E 6BT, United Kingdom

<sup>4</sup>Department Chemie, Universität München, Butenandtstraße 5-13 E, 81377 München, Germany

(Received 23 July 2002; revised manuscript received 11 September 2002; published 27 December 2002)

By combining experimental dynamic scanning force microscope (SFM) images of the  $\text{CaF}_2(111)$  surface with an extensive theoretical modeling, we demonstrate that the two different contrast patterns obtained reproducibly on this surface can be clearly explained in terms of the change of the sign of the electrostatic potential at the tip end. We also present direct theoretical simulations of experimental dynamic SFM images of an ionic surface at different tip-surface distances. Experimental results demonstrate a qualitative transformation of the image pattern, which is fully reproduced by the theoretical modeling and is related to the character of tip-induced displacements of the surface atoms. The modeling of the image transformation upon a systematic reduction of the tip-surface distance with ionic tips allows an estimate of the tip-surface distance present in experiment, where 0.28–0.40 nm is found to be optimal for stable imaging with well-defined atomic contrast. We also compare the modeling with ionic tips to results for a pure silicon tip. This comparison demonstrates that a silicon tip can yield only one type of image contrast and that the tip-surface interaction is not strong enough to explain the image contrast observed experimentally. The proposed interpretation of two types of images for the  $\text{CaF}_2(111)$  surface can also be used to determine the chemical identity of imaged features on other surfaces with similar structure.

DOI: 10.1103/PhysRevB.66.235417

PACS number(s): 68.37.Ps, 07.05.Tp, 68.35.Bs, 07.79.Lh

## I. INTRODUCTION

Dynamic scanning force microscopy (dynamic SFM) (Ref. 1) is a powerful technique for atomically resolved imaging of a wide variety of insulating,<sup>2–5</sup> semi-insulating,<sup>6–11</sup> and van der Waals surfaces,<sup>12</sup> as well as for the highest resolution imaging of molecular species on surfaces.<sup>13–15</sup> However, details of the mechanism of contrast formation and chemical identities of observed image features often remain unresolved. This is mainly due to the fact that the tip-surface interaction probed in dynamic SFM is determined by the details of the tip atomic structure, which is very difficult to establish directly. Understanding the various factors important in resolution requires a direct comparison of theoretical models with experimental images obtained with different tips and at different tip-surface separations. The aim of this paper is to test some of the long existing assumptions of theoretical modeling of dynamic SFM on ionic surfaces, which are crucial for an unambiguous interpretation of experimental images and for providing a complete interpretation of images on surfaces such as  $\text{CaF}_2$ .

One of these assumptions concerns the tip atomistic structure. Common experimental procedures for tip preparation often include  $\text{Ar}^+$  sputtering of oxidized silicon tips, and intentional or unintentional contact with the surface under study. Hence, tips can be covered by a native oxide, residual water, and/or constituents of the surface, and it has been suggested to model tips by clusters of ionic material at the tip end.<sup>16,17</sup> An alternative model commonly employed in a number of theoretical studies is that of a silicon tip with one or two dangling bonds at the terminating silicon atom.<sup>18–21</sup>

This model appears to be more appropriate for imaging silicon surfaces where tips can be contaminated or deliberately covered by silicon clusters.<sup>22</sup>

The ionic tip model implies that the image contrast is not determined by covalent tip-surface interactions, but mainly by the interaction of the tip with the surface electrostatic potential. To achieve atomic resolution, tips should have some atomically sharp feature at the end.<sup>23</sup> Since this feature can be terminated by either a positive or a negative ion, image contrast may strongly depend on termination. In fact, it has been demonstrated theoretically for ionic surfaces that the sign of the electrostatic potential of the tip determines which surface sublattice is imaged as bright.<sup>4,23,24</sup> To prove this conjecture requires an unambiguous demonstration that two different types of images obtained on the same surface are due to two differently terminated tips, and distinguishing that from other unique rearrangements of tip atoms which do not change the sign of the tip potential. As the real tip structure is unknown, this is impossible to achieve on highly symmetric surfaces of simple cubic materials like  $\text{NaCl}$ .<sup>23</sup> Previous studies on the  $\text{CaF}_2(111)$  surface demonstrated that high quality experiment and theory can be combined to provide unambiguous interpretation for characteristic contrast patterns reproducibly obtained when scanning with a certain tip.<sup>4,17</sup> These studies established that the contrast pattern for this system strongly depends on the atomic structure of the tip and on the tip-surface distance. Theory predicts that with a net positive electrostatic potential from the tip, images exhibit a triangular contrast pattern, characterized by the positions of maxima over the fluorine ions, in quantitative agreement with the experimental data.<sup>17</sup> Here we complete the study, and demonstrate that the two contrast patterns

obtained reproducibly on this surface can be clearly explained in terms of a change of the sign of the tip electrostatic potential.

These results do not prove, but strongly suggest, that the tip is covered by oxide or a  $\text{CaF}_2$  cluster, and support the idea that the sign and gradient of electrostatic potential of the tip are crucial for image contrast on ionic surfaces. This still leaves a possibility that the tip is terminated by pure silicon. To investigate whether this model could also explain the experimental images of the  $\text{CaF}_2(111)$  surface, we carried out extensive quantum mechanical calculations of the tip-surface interaction. Results clearly demonstrate that a silicon tip could be responsible only for one type of image contrast and the silicon tip-surface interaction is not strong enough to explain the observed image contrast.

Tip-induced surface distortion has been identified as an important component of the mechanism of contrast formation of insulator and semiconductor surfaces,<sup>16,21–23,25,26</sup> but direct observation of atomic displacements is impossible and such theoretical predictions remain unconfirmed. However, it has been demonstrated that atomic displacements strongly depend on the tip-surface separation and their influence on image patterns should depend on the smallest tip-surface distance in the course of tip oscillations.<sup>4</sup> In this paper we present direct theoretical simulations of experimental dynamic SFM images of an ionic surface at different tip-surface distances. Experimental results demonstrate a qualitative transformation of the image pattern, fully reproduced by the theoretical model. Theory shows that this transformation is directly related to the character of tip-induced displacements of surface atoms, and this provides strong evidence of the importance of ionic displacements in image formation.

The absolute tip-surface distance cannot be directly measured experimentally, and generally it has been assumed that the shortest tip-surface distances achieved in dynamic SFM are far from “hard contact.” However, notions of contact and distance in this context are ill defined due to strong chemical interactions and dynamic relaxation involved. In general, experiments show that one needs to achieve a very small tip-surface distance to resolve surface features. Previous modeling suggested, however, that instabilities of surface and tip ions caused by the tip-surface interaction at short distances can lead to tip contamination and image changes,<sup>27</sup> and that these effects depend on tip and surface chemical structures. Again, a direct comparison of experimental images at different tip-surface distances with theoretical simulation may help to determine real distances involved in these measurements. Results presented here demonstrate that strong displacements of tip and surface ions can have reversible character and the stability of the dynamic SFM operation can be preserved, even when approaching the surface to 0.275 nm.

To elucidate in detail the questions outlined above, we discuss the experimental and theoretical methods in the Sec. II, while in Sec. III we present results of simulations and experimental images mainly representing the  $\text{Ca}^{2+}$  sublattice in contrast to our previous work focused on imaging the  $\text{F}^-$  sublattice.<sup>4,17</sup> In Sec. IV we discuss the results of measurements and simulations for different tip-surface distances.

Section V is focused on modeling the interaction of a silicon tip with the  $\text{CaF}_2(111)$  surface, and all the results are summarized in Sec. VI. In the synopsis of the results we develop a complete picture of the contrast mechanisms for this system, and also explore the limits of comparison between experiment and theory. Based on this understanding and using the unique image features predicted and observed for this system, we establish  $\text{CaF}_2(111)$  as a *reference* surface and tool for the calibration of tips in atomic resolution dynamic scanning force microscopy.

## II. METHODS

This work is based on experimental and theoretical methods described previously,<sup>4,16</sup> and in this section we only briefly revisit the main features relevant to the following discussion. Experiments were performed with a commercial scanning force microscope operated in the dynamic mode<sup>28</sup> and in an ultrahigh vacuum system with a base pressure in the low  $10^{-8}$  Pa range. We used cantilevers with a resonance frequency between 60 and 80 kHz, and a spring constant between 3 and 7 N/m. With respect to the dynamic mode of the force microscope, an important feature is that we scan in constant height mode, i.e., at a fixed tip-surface distance with only slow adjustment (low gain in the distance feedback control loop) to compensate for an inclination between imaging and surface planes.<sup>4</sup> Images are recorded in the forward and backward directions sequentially line by line during one complete scan of the surface. The influence of the distance and amplitude control loops has been checked by an extended series of measurements involving a systematic variation of scan speed and feedback loop gain. We found that none of the contrast features discussed here is artificially created by these loops.

Simulations were performed with a model for all relevant interaction forces, including *microscopic* chemical forces between ions or atoms at the tip end and surface ions, and *macroscopic* van der Waals force between tip and surface. Electrostatic forces due to work function differences, charging and polarization were also explored, but were found to be negligible in this system in accordance with the experimental procedure of compensating charges by a properly chosen bias voltage. We explore two types of tip models that require different treatments of the tip-surface interaction. To model a tip covered by ionic material, such as a native oxide layer or a  $\text{CaF}_2$  cluster adsorbed at the end of the tip, we use a 64-atom  $\text{MgO}$  cube embedded into the macroscopic tip that is represented as a conducting cone with a spherical apex.<sup>16</sup> The cube can be oriented with either a  $\text{Mg}^{2+}$  or  $\text{O}^{2-}$  ion at the apex, producing either a local positive or negative electrostatic potential at the tip end, respectively. This was previously shown to qualitatively represent the potential of oxidized or contaminated silicon tips and ionic clusters,<sup>29</sup> and has demonstrated good comparison with experiment on several systems.<sup>4,23,30</sup>

In this model, chemical forces are calculated using a periodic atomistic simulation technique and the MARVIN2 code.<sup>31</sup> The empirical parameters used for the tip,  $\text{CaF}_2$  surface and tip-surface interactions are the same as in Ref. 4.

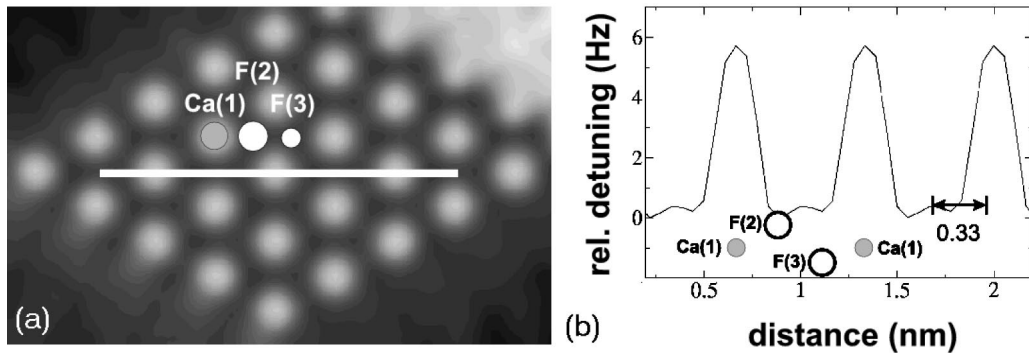


FIG. 1. (a) Simulated image and (b) cross section for a tip with a negative electrostatic potential scanned at a height of 0.350 nm. The white line in the image is along the  $\langle \bar{2}11 \rangle$  direction and indicates the position of the cross section. Labels refer to ions from different sublattices. Fluorine ions in the upper surface layer are denoted as high  $F^-$  ions [F(2)] and those in the third surface layer as low  $F^-$  ions [F(3)]. The calcium layer [Ca(1)] in between the fluorine layers is the reference plane for the tip height.

The surface periodic cell is a cubic cluster of  $6 \times 6 \times 3$   $\text{CaF}_2$  units, as in our previous work.<sup>4</sup> In the simulation, 44 atoms of the nanotip closest to the surface and the top two layers of the surface were allowed to relax with respect to interatomic forces.

Two distinctly different atomic image patterns discussed in this paper have been obtained reproducibly using different tips. Since these image patterns do not depend on the van der Waals contribution to the force from the macroscopic part of the tip, throughout this work we use the same parameters of the van der Waals interaction between the conical macroscopic part of the tip and the surface. These have been obtained by fitting our model to one set of experimental force vs distance curves<sup>4,32,33</sup> in the long range interaction region, assuming a Hamaker constant of 1 eV (Ref. 34) and a negligible electrostatic contribution.

Although it is common experimental practice to bring tips into contact with the surface prior to measurements, carefully prepared, clean silicon tips are also an option for imaging and might yield images of a different contrast, where the role of covalent tip-surface interactions are significant. Therefore, it is useful to explicitly calculate the interactions of a clean silicon tip with the surface. For this study we must use more complex theoretical methods to model the tip and tip-surface interactions. These calculations have been performed using the linear combination of atomic orbitals basis SIESTA code,<sup>35,36</sup> implementing the density functional theory with the generalized gradient approximation, and the functional of Perdew, Burke, and Ernzerhof known as PBE.<sup>37</sup> Core electrons are represented by norm-conserving pseudopotentials using the Troullier-Martins parametrization.<sup>36</sup> The pseudopotential for the silicon atom was generated in the electron configuration  $[\text{Ne}]3s^23p^2$ , calcium in  $[\text{Ar}]4s^2$ , and that for fluorine in  $[1s^2]2s^22p^5$ , where square brackets denote the core electron configurations.

In the final stage of modeling, the microscopic and macroscopic forces are combined, and the cantilever oscillations are simulated under the influence of the full tip-surface interaction as in earlier studies.<sup>16</sup> To match the experimental procedure, simulated images are calculated in the constant height mode as outlined in the previous section.

### III. STANDARD IMAGES

Previous studies considered only a full theory versus experiment comparison of images for a positively terminated tip at one tip-surface separation.<sup>4,17</sup> In this section the comparison is extended to results for tips with negative termination, as predicted by theory and now clearly observed also in experiment.

We first discuss properties of simulated images at a single height and compare them directly with experiment. Height refers to the distance between the unrelaxed tip terminating atom and the unrelaxed  $\text{Ca}^{2+}$  sublattice in the lower turning point of the oscillation. Simulated images discussed in this section were produced for a tip height of 0.350 nm. At this height, the simulated contrast matches the experimental average contrast, demonstrating a comparable interaction strength. Note, however, that the interaction ranges strongly depend on the true microscopic tip in an experiment, and any references to distance based on contrast at one height can only be considered as an estimate. The accuracy of height estimates will be developed in a later section.

Figure 1(a) shows a simulated image and scanline obtained with a negative potential tip at a 0.350-nm height. The image demonstrates a clear circular or “disklike” contrast with strongest brightness centered on the position of the  $\text{Ca}^{2+}$  ions in the surface [Ca(1) in Fig. 1]. The scanline shows that contrast is dominated by a large peak over the  $\text{Ca}^{2+}$  ion, with a much smaller peak in between the high and low fluorine ions. The smaller peak is due to a minimum in repulsion between the tip and  $F^-$  ions; however, this peak is so small in comparison to the main peak over Ca that it has no visible effect on the contrast pattern in images.

The domination of  $\text{Ca}^{2+}$  ions in the negative potential tip contrast pattern has two components: (i) The positive surface potential over the  $\text{Ca}^{2+}$  ions has a strong attractive interaction with the negative potential from the tip. Figure 2(a) clearly shows the domination of the attractive interaction over the  $\text{Ca}^{2+}$  ions. (ii) As the tip approaches the surface, the  $\text{Ca}^{2+}$  ions displace toward it and the  $F^-$  ions are pushed into the surface. Figure 2(b) shows that, at 0.350 nm over the Ca(1) site, the  $\text{Ca}^{2+}$  ion displaces by 0.118 nm outward, also

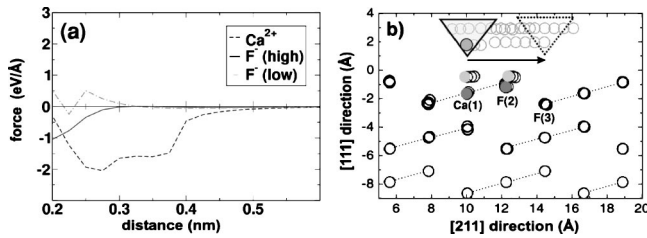


FIG. 2. Theoretical data from simulations with a negative electrostatic potential tip: (a) chemical force curves over the Ca and high and low F atomic sites; (b) full trajectories of atoms in a plane as the tip follows the  $\langle\bar{2}11\rangle$  scanline at a height of 0.350 nm. Labels Ca(1), F(2) and F(3) are as in Fig. 1. The atoms shaded light gray in the surface indicate initial positions of the most relevant atoms when the tip is over Ca(1) (leftmost tip position in figure), whereas atoms shaded dark gray are final positions when the tip is over F(3) (rightmost position). Note that trajectories of only the bottom four atoms (one  $O^{2-}$  ion and three  $Mg^{2+}$  ions) of the tip have been included.

forcing the high  $F^-$  ion outward. However, as the tip moves toward the F(2) site, the  $Ca^{2+}$  ion drops back to the surface and the high  $F^-$  ion is actually pushed in by 0.027 nm. The low  $F^-$  ions [F(3)] are not displaced significantly from their equilibrium positions at this scanning height. Displacement of ions from the surface greatly increases the range of the local surface electrostatic potential<sup>16</sup> and increases tip-surface interaction. In principle, a displacement of the tip ions will also cause similar effects, however, the hardness of MgO in comparison to  $CaF_2$  means that the tip ions do not displace significantly. Note that in Fig. 2(b) the atom trajectories represent snapshots from a static simulation. In a real experiment the tip will oscillate for many cycles at a given position, and the average interaction is measured—hence the modeling approximates this average interaction with a single static calculation at each tip position, rather than trying to simulate the full dynamic process.

In most experiments, the tip is not highly symmetric as it is assumed for simulation. Tip asymmetry often results in atomic contrast differences in simultaneously recorded images along forward and backward scanning directions, and to distortions within an image with respect to the real surface symmetry. Figure 3 illustrates this case by showing images for both scanning directions. These images clearly represent the main features predicted by simulations for a tip with negative termination. The contrast details, however, differ significantly from the standard contrast pattern. Bright features in the image of the forward direction ( $\Rightarrow$ ) appear as sharp spots with an additional dark spot next to them whereas the image in the backward direction ( $\Leftarrow$ ) exhibits an apparent duplication of features and they seem to be more elongated and broader than those found in forward direction. The apparent distortion of surface symmetry can be seen in cross sections along equivalent  $\langle\bar{2}11\rangle$  directions taken from the image in backward direction ( $\Leftarrow$ ) and displayed on the right side of Fig. 3. The shape and relative height of the smaller peaks in between the large ones appear as significantly different when cross sections 1, 2, and 3 taken in equivalent directions are compared to each other. The large

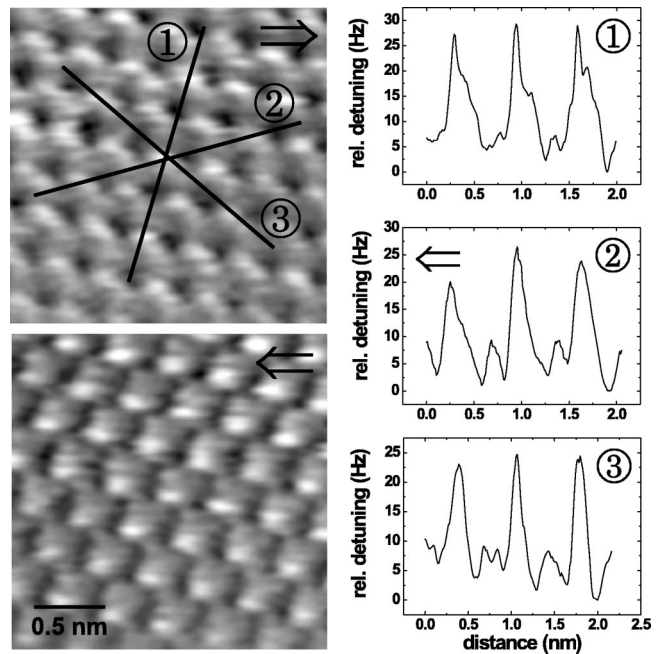


FIG. 3. Experimental images and scanlines recorded with an asymmetric tip. The images have been recorded along forward ( $\Rightarrow$ ) and backward ( $\Leftarrow$ ) scanning directions. The frames on the right represent scanlines of the three equivalent  $\langle\bar{2}11\rangle$  directions, and have been taken from the image in the backward direction. The measurement was gained at a mean frequency detuning of  $-146$  Hz and with an oscillation amplitude of 35 nm.

peaks in cross-section 1 are broader and appear as split, unlike that found in the cross-sections along the other directions. Previous calculations of asymmetric<sup>38</sup> and rotated<sup>30</sup> MgO tips demonstrated the sensitivity of contrast formation to tip orientation and structure. However, a detailed understanding of the directional dependence of contrast in some images is beyond the current model, and is the subject of future study.

Careful tip preparation in the form of a repeated, gentle contact between tip and surface can lead to tips which have a highly symmetric sensing cluster at the end. As an example for a measurement with a symmetric tip, in Fig. 4 we show contrast patterns that are close to perfect in terms of the standard image from Fig. 1. The recorded images along both scanning directions exhibit exactly the same contrast features of bright ions appearing as disks, and along equivalent  $\langle\bar{2}11\rangle$  directions the same contrast features can be identified except for minor discrepancies in the relative height of the smaller maximum.

We immediately see a clear qualitative and quantitative agreement between experiment and theory. The smaller peak is predicted from modeling to appear at a distance of 0.330 nm from the main peak over the  $Ca^{2+}$  sublattice. If we take over 70 experimental cross sections from images, we find that the average position of the small peak is  $0.320 \pm 0.050$  nm, in excellent agreement with theory. Furthermore, the predicted peak-to-valley contrast of 6 Hz is found in experiments. Combining these results with the previous quantitative agreement for the triangular contrast pattern<sup>4,17</sup>

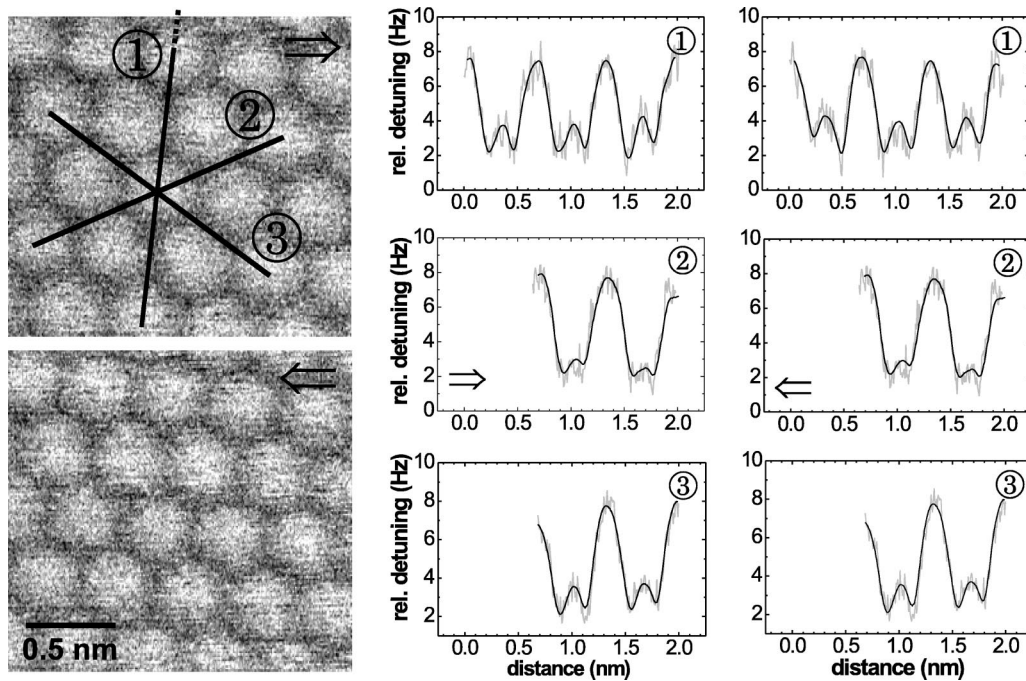


FIG. 4. Experimental images and scanlines recorded with a symmetric tip demonstrating “disklike” contrast. The images have been recorded in forward ( $\Rightarrow$ ) and backward ( $\Leftarrow$ ) scanning directions and the scanlines have been taken along the three equivalent  $\langle \bar{2}11 \rangle$  directions (1), (2) and (3) from both images. The measurement was gained at a mean frequency detuning of  $-83$  Hz and with an oscillation amplitude of  $48$  nm.

demonstrates that full interpretation has been achieved for the two contrast patterns consistently seen in atomically resolved images of  $\text{CaF}_2(111)$ .

#### IV. DISTANCE DEPENDENCE OF CONTRAST FORMATION

Since we have demonstrated both qualitative and quantitative agreement between experiment and theory at a certain tip height, it is interesting to explore whether agreement is preserved for a range of heights. Figures 5(a)–5(c) show experimental images at increasing average frequency detuning i.e., reduced height. Figures 5(a) and 5(b) clearly show the triangular contrast characteristic of imaging the fluorine sublattice, although slight variations in image contrast can be seen in both frames. Persistence of this pattern in experimental images obtained under different conditions shows that the triangular contrast pattern is not a unique feature seen only at a specific height, but is rather a distinct pattern related to the sign of the tip potential. However, in the image corresponding to closest approach, we see that the contrast pattern changes considerably. Figure 5(c) shows a honeycomb pattern, with all  $\text{F}^-$  sites now completely linked in bright contrast.

To understand whether this very distinct change in contrast could be explained within the same model as discussed in Sec. III, we performed further extensive modeling. Figures 5(d)–5(h) show the development of contrast in simulated images as the scanning height is reduced. Figure 5(d) demonstrates that even at the very large distance of  $0.500$  nm the triangular contrast pattern is present. It is unlikely, however,

that the small chemical forces acting at this tip-surface distance could be detected by room temperature experiments. As the tip approaches the surface [Figs. 5(e) and 5(f)], theory predicts that the triangular pattern becomes more vivid, as seen in the experimental images. At a  $0.275$ -nm tip height, simulated images develop the honeycomb contrast pattern, as shown in frame (g), that nicely corresponds to the observed contrast in the closest approach experimental image Fig. 5(c). In frame (h) corresponding to a  $0.250$ -nm tip height, the honeycomb pattern develops some internal structure, however, this will most probably not be accessible by experiment as tip instability is expected to occur for this small tip-surface distance.

Further agreement between experiment and simulation can be seen by comparing the systematic change in experimental and theoretical scanlines upon reducing the tip-surface distance. Figures 6(a) and 6(b) show that for large tip-surface separation, both experimental and theoretical curves exhibit the large peak/small shoulder feature characteristic for the triangular contrast pattern. However, as the tip approaches the surface, the magnitude of the shoulder increases until, for scanlines from the honeycomb images, it is clear that the shoulder is at least equal to the original main peak. In fact, scanlines from experimental closest approach show that the shoulder is larger than the main peak, a feature which occurs in the simulated scanlines at a distance of  $0.250$  nm. Also note that, despite the simplistic tip model, the magnitude of contrast as a function of distance in experiment and theory agrees well. Over an experimental average detuning change of  $-19$  Hz [Figs. 6(a)–6(c)] the average contrast changes from about  $4$ – $10$  Hz, whereas theory predicts a

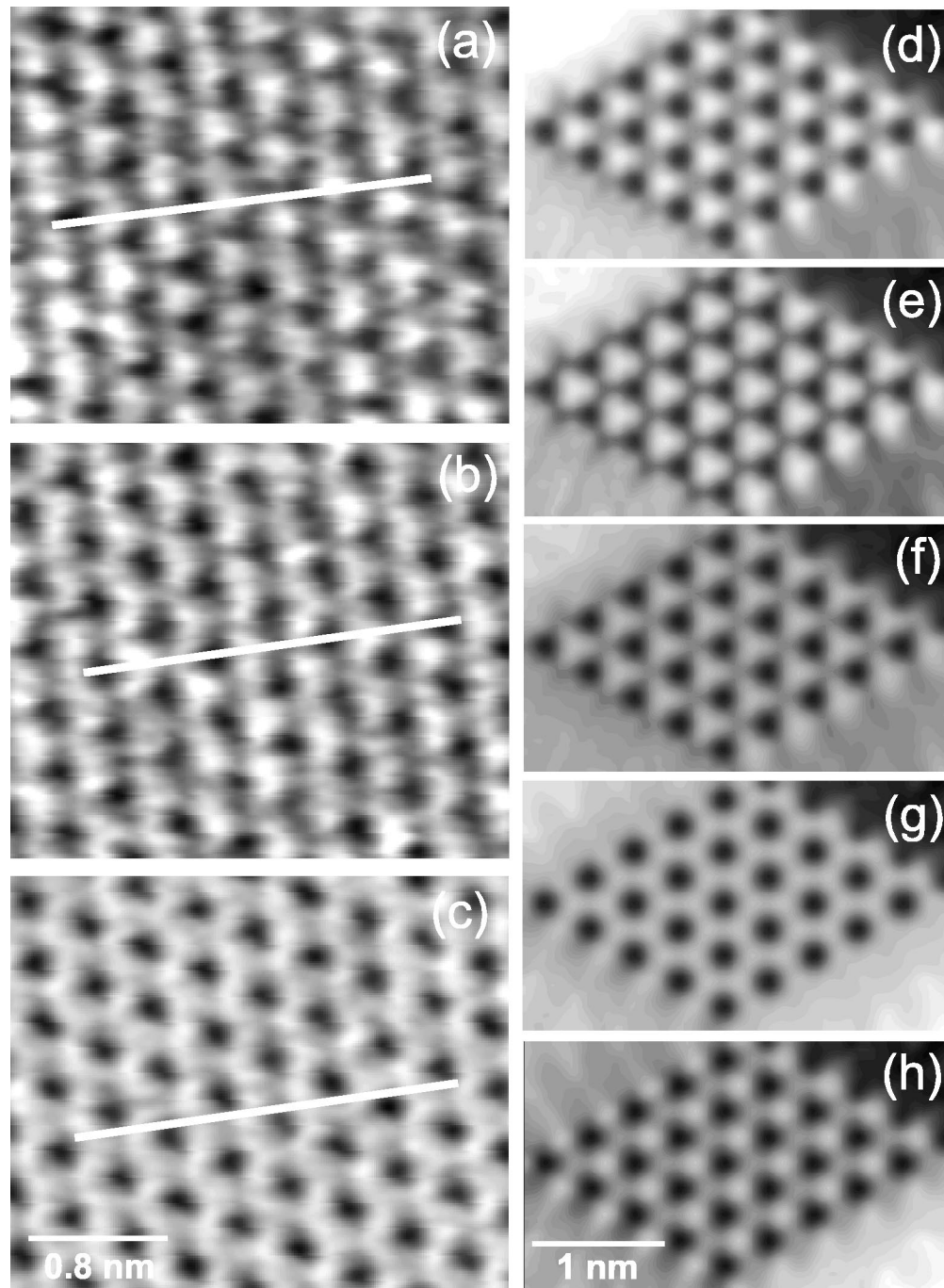


FIG. 5. (a)–(c) Experimental images taken as the tip approaches the surface (Ref. 4) by increasing the mean detuning ( $-121$ ,  $-127$ , and  $-140$  Hz). (d)–(g) Simulated images at  $0.500$ ,  $0.375$ ,  $0.325$ ,  $0.275$  and  $0.250$  nm using a positive potential tip. The scale of the images is shown in Fig. 6.

change from  $4$ – $7$  Hz contrast for a change of  $-26$  Hz in average detuning [Figs. 6(e)–6(h)]. This suggests that there is good correspondence in the increase of strength in interaction as a function of distance.

A more thorough understanding of this agreement in contrast development requires studying in detail the changes in forces and atomic displacements as the tip approaches the surface. Figure 7(a) gives the chemical force over the relevant sites in the  $\text{CaF}_2$  surface as a function of distance for a tip with positive termination. For distances larger than

$0.400$  nm, the curves are as one would expect them, i.e., we find repulsion over the positive  $\text{Ca}^{2+}$  ion and attraction above the  $\text{F}^-$  ions. Note, however, that when the macroscopic van der Waals interaction is included, *the overall tip-surface interaction is always attractive*, as is required for stable dynamic SFM operation. From the ionic interaction, we find some attraction over the low  $\text{F}^-$  ion and stronger attraction over the high  $\text{F}^-$  ion. Moving closer than  $0.400$  nm, we observe that the attraction over the high  $\text{F}^-$  ions reduces and increases over the low  $\text{F}^-$  sites, until

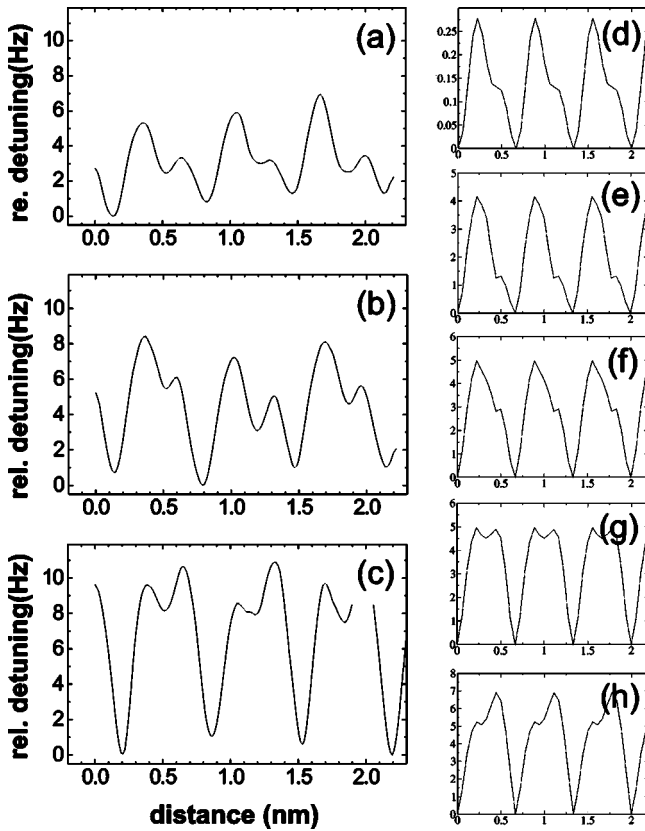


FIG. 6. Comparison of (a)–(c) experimental and (d)–(h) simulated scanlines taken at the positions of white lines from the images in Fig. 5.

around 0.320 nm the greatest attraction is now over the low  $F^-$  site. This behavior can be understood by looking at atomic displacements as the tip approaches. At 0.350 nm there is strong displacement of the high  $F^-$  ion [F(2)] toward the tip [see Fig. 7(b)], producing a very strong attractive interaction, however, as the tip moves closer, this  $F^-$  ion is driven back into the surface and the force is reduced. Frame (c) shows that the high  $F^-$  ion has been pushed effectively back into its original lattice position at a tip-surface separation of 0.250 nm. However, when the tip is over the low F(3) site, we see very little movement of the closest high  $F^-$  ion, but in fact, aided by the proximity of the  $Ca^{2+}$  ion, there is a much smaller barrier for displacement of the high  $F^-$  ion from the next nearest row [ion F(4)]. Frame (d) shows how the next nearest high  $F^-$  ion displaces very strongly to the tip at 0.325 nm when it is over the F(3) site.

In summary, at a distance of 0.500 nm the interaction with the high  $F^-$  atom dominates, and we see only relatively small shoulders in scanlines over the low  $F^-$  sites. As the tip approaches, the nearest high  $F^-$  ion is pushed into the surface, reducing its dominance, and the interaction with the low  $F^-$  and the next nearest high  $F^-$  ion increases the relative size of the shoulder. This corresponds to the increasing vividness of the triangular contrast pattern in images. Finally, the contribution from the high  $F^-$  ion is balanced by the contribution from the low  $F^-$  /next high  $F^-$  ion, and the main peaks and shoulders are equivalent in scanlines, and it

is this equivalence which produces the characteristic honeycomb contrast pattern.

Simulated images produced at tip-surface distances lower than 0.275 nm actually predict that a quasitriangular contrast pattern will reappear; however, the orientation of the triangles would then be reversed. Interaction over the low  $F^-$  sites would dominate, and it is over the high  $F^-$  sites that the smaller shoulders would appear. As yet this type of contrast pattern change has not been observed in experiments on  $CaF_2$  and might never be observable as severe tip instability is likely to occur at such a small tip-surface distance.

## V. IDEAL SILICON TIP

In this section, we extend the discussion to a nonionic tip, which is modeled by pure silicon. On more reactive, semi-conducting surfaces, it has been shown that for a pure silicon tip, contrast is dominated by the onset of bonding between dangling bonds in the tip and surface,<sup>18,22</sup> and such bonding was recently explored in detail experimentally.<sup>39</sup> Here we explore how this kind of tip interacts with an ionic surface.

To represent a pure silicon tip, we use a ten atom silicon cluster, with its base terminated by hydrogen. This has been shown previously<sup>19,22</sup> to provide a good model of a clean silicon tip with a single dangling bond at the apex. The smaller size of the silicon cluster compared to the  $MgO$  cube allows us to use a correspondingly smaller surface size, and the crystal is here simulated by a cluster of  $4 \times 4 \times 3$   $CaF_2$  units. The bottom two layers of the tip and the top two layers of the surface are allowed to relax with respect to atomic forces, as in the previous simulations.

Figure 8 shows calculated tip-surface forces as the silicon tip approaches the  $Ca^{2+}$ , high  $F^-$ , and low  $F^-$  sites in the  $CaF_2$  surface. It is clear that contrast in images with a silicon tip would be dominated by interaction with the high  $F^-$  sublattice, and to a lesser extent the low  $F^-$  sublattice. The interaction with  $Ca^{2+}$  is much weaker, and enters repulsion at larger tip height (about 0.330 nm) than over the  $F^-$  sites (about 0.250 nm). The interaction between the tip and the  $F^-$  ions is due to the onset of covalent bonding between Si and  $F^-$ , involving charge transfer from the  $F^-$  ions into bonding states. At a 0.300-nm tip height, the charge transfer is  $0.18e$  for the high  $F^-$  ion, but only  $0.02e$  for the low  $F^-$  ion (based on Mulliken population analysis<sup>40</sup>). Over Ca, there is no charge transfer until small heights (about 0.300 nm), where charge is actually transferred from the neighboring high  $F^-$  site to the tip. However, at this point the tip has already entered the repulsive interaction region and the effect is negligible.

If we now compare the silicon tip force curves with those in Fig. 7(a), we see qualitatively the same behavior in the range between 0.300 and 0.500 nm: a very weak interaction beyond 0.450 nm, the largest interaction over high  $F^-$ , the weakest interaction over  $Ca^{2+}$ , and low  $F^-$  somewhere between. Note that the onset of repulsion over the  $Ca^{2+}$  site even occurs at qualitatively the same position as in Fig. 7(a), at the maximum in attraction over the high  $F^-$  site. This agreement implies that a pure silicon tip could only produce a triangular contrast pattern, as for the positive potential

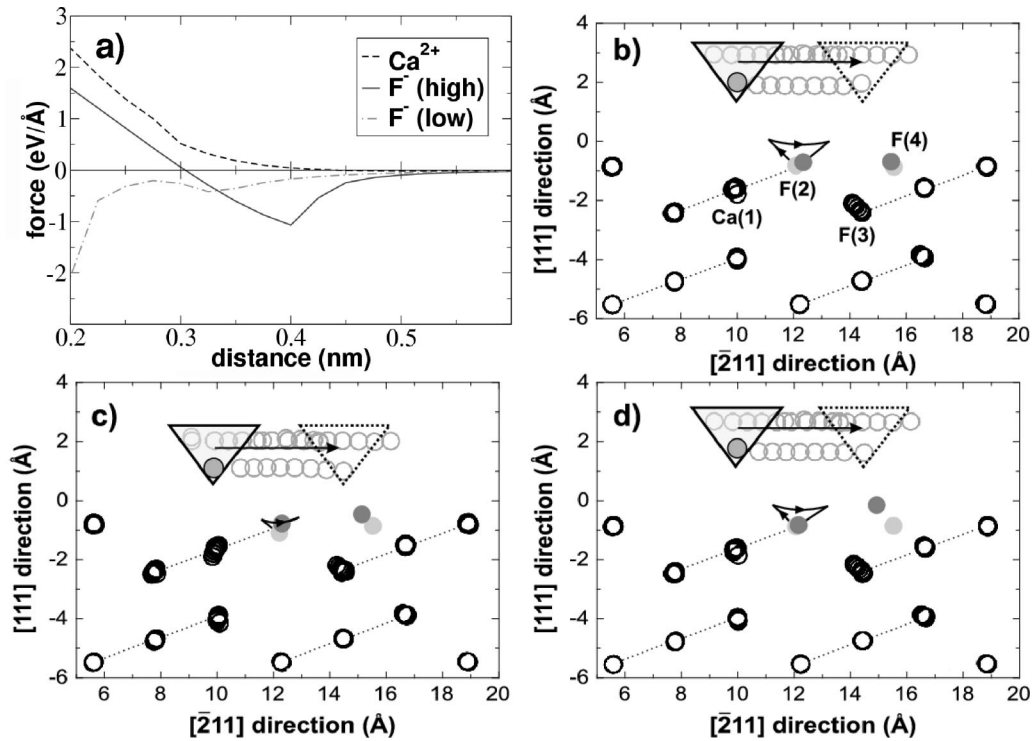


FIG. 7. Theoretical data from simulations with a positive electrostatic potential tip: (a) chemical force curves over the Ca, high and low F atomic sites; full trajectories of atoms in a plane as the tip follows the  $\langle \bar{2}11 \rangle$  scanline. The tip-surface distances are (b) 0.350 nm, (c) 0.250 nm, and (d) 0.325 nm. Labels Ca(1), F(2), and F(3) are as in Fig. 1. The atoms shaded light gray indicate initial positions of the most relevant atoms when the tip is over Ca(1) (leftmost tip position in figure), whereas atoms shaded dark gray are final positions when the tip is over F(3) (rightmost position). F(4) is a high fluorine atom out of the plane, but its trajectory has been projected on to the same plane as the other atoms for clarity. Note that trajectories of only the bottom four atoms (one  $\text{Mg}^{2+}$  ion and three  $\text{O}^{2-}$  ions) of the tip have been included.

ionic tip at medium to long range. At smaller ranges, the differences in force for the ionic tip are due to the strong displacements induced by the tip approach, in agreement with experiment (see Sec. IV). Note that, for the silicon tip, interaction forces are considerably smaller than for the ionic tip and, therefore, displacements for a pure silicon tip are much smaller. Over the  $\text{Ca}^{2+}$  ions, there is almost no surface ion displacement until very small tip-surface separations when the  $\text{Ca}^{2+}$  directly underneath the tip is pushed in. Over the high  $\text{F}^-$  site, at 0.350 nm the  $\text{F}^-$  ion under the tip is at a maximum displacement of 0.040 nm toward the tip, before being pushed back in. There is no significant displacement of the low  $\text{F}^-$ , or any atoms not directly underneath the tip. Due to the softness of the silicon tip in comparison to the ionic MgO tip, tip atom relaxations play a more significant role in the interaction. Over the high  $\text{F}^-$  there is no significant displacement of the apex Si atom toward the surface, but at a 0.300-nm tip height it is displaced by 0.025 nm into the tip due to strong repulsion from the proximity of the  $\text{F}^-$ . Over the  $\text{Ca}^{2+}$  ion a similar process occurs, but the tip apex displacement at the same height is only 0.010 nm. These tip atom relaxations slightly reduce the overall tip-surface interaction, but would have no significant influence on images due to their short-range and small magnitude. However, it is possible that for other, even softer, tips, this contribution could be relevant in contrast formation.

Comparing the magnitude of force curves for the two different tips, we recognize immediately that the force between a pure silicon tip and the  $\text{CaF}_2$  surface is much less than for a positive potential ionic tip. At first sight, one might expect that there is a strong interaction between Si and F, as F is a very reactive species. However, in this case we are effectively dealing with  $\text{F}^-$  ions with a full outer shell, not atoms, and there is no possibility of the large charge transfer characteristic of Si and F interacting in atomic form. If we calculate the maximum possible contrast for a pure silicon tip imaging  $\text{CaF}_2$ , it is about 2 Hz—several times smaller than that seen for simulations with an ionic tip, and, more signifi-

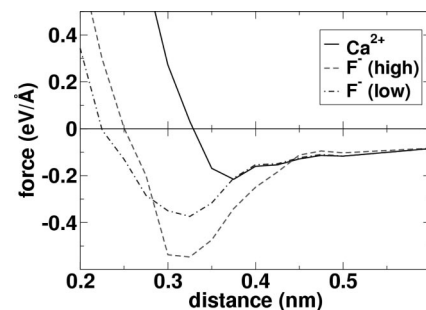


FIG. 8. Simulated force curves taken over the Ca, high and low F sites in the  $\text{CaF}_2$  (111) surface with a pure silicon tip.

cantly, in experiments. This is a consequence of both the weaker attraction to the  $F^-$  ions, and the lack of medium-range repulsion over  $Ca^{2+}$  ions, reducing the overall contrast.

## VI. DISCUSSION

Although interpretation of dynamic SFM measurements remains far from trivial, we have shown that by combining experiment and theory a significant understanding can be achieved even from simple models. By representing two example ionic tips, with opposite signs of the electrostatic potential at the apex, it is possible to interpret a wide variety of contrast patterns seen in different experiments, with different tips and at different scanning heights. The agreement seen, in contrast patterns and contrast magnitude, between theory and experiment as the tip approaches the surface, encourages the use of theory as a reference for distance in experiments. Although utmost accuracy will always depend on a precise modeling of the tip, the distance dependence of surface deformations and contrast patterns can be well reproduced with simple tip models.

An overall comparison of the ionic and silicon tip models suggests that the ionic tip model clearly provides a more consistent agreement with available experiments on the  $CaF_2(111)$  surface. In particular, the magnitude of possible contrast predicted with the silicon tip is much smaller than seen in experiments. In additions, the nature of the silicon force curves implies that only the triangular contrast pattern could be imaged with the same tip. Tip contamination (by, for example, fluorine) would be required to explain disklike (and other) contrast patterns. This is an important result, since the experimental practice of using unspattered tips and bringing them into contact with the surface before imaging surely prohibits a clean silicon tip in most cases. A theoretical modeling demonstrates that the sign of the electrostatic potential of the nanocluster at the tip apex is crucial in determining the contrast pattern.

Assuming the validity of the ionic tip model, we observe strong displacements of the surface ions, which significantly contribute to image contrast formation. These displacements are of the order of the tip-surface separation (defined with respect to the frozen tip and surface) already at relatively large tip-surface distances of about 0.350 nm. This blurs the notion of tip-surface distance and suggests a much more dynamic picture of the contact area. We consider the very good agreement of different image patterns at different frequency detuning values predicted theoretically and obtained experi-

mentally as a strong confirmation of this model, and of the existence of ion displacements. Note, however, that the simulations are performed at 0 K, and the real displacements of the tip and surface atoms will depend on temperature. The dynamic picture would be much more colourful, similar to that discussed in Refs. 24, 27, and 41, although it may not give any deeper insight into the contrast mechanisms. It is also interesting to note that the complex surface deformations seen with an ionic tip are not present for a silicon tip. Instead we observe stronger tip atom displacements at short tip-surface distances.

We should also note that the *ab initio* results obtained with the silicon tip are, to our knowledge, the first of this kind on ionic surfaces—they demonstrate a quite significant electron density transfer between the tip and the surface contributing to the strength of the tip-surface interaction. This interesting and important result should be much more pronounced on other surfaces with smaller band gaps.  $CaF_2$  has one of the widest band gaps of about 12 eV, and hence a relatively large band offset of the fluorine valence band and the conduction band of silicon. Most insulators have much smaller gaps and band offsets, and are expected to exhibit a much larger electron transfer. This, in turn, should lead to much stronger tip-surface interaction. For thin insulating films on metal substrate this effect can be controlled by an applied voltage,<sup>42</sup> and, therefore, it might be extremely interesting to study the voltage dependence of image contrast on these systems using conductive silicon tips.

Finally, we point out that the unprecedented level of detailed understanding of dynamic SFM imaging of the  $CaF_2(111)$  surface and the relative ease of its preparation suggests that it can be used as a reference for determining tip polarity, studying molecular adsorption and manipulation. The proposed interpretation of two types of images for the  $CaF_2(111)$  surface can also be used to determine the chemical identity of imaged features on other surfaces with similar structure.<sup>11</sup>

## ACKNOWLEDGMENTS

This research was supported by the Academy of Finland through its Centres of Excellence Program (2000-2005). A.S.F. wishes to thank the Center for Scientific Computing, Helsinki for use of its computational resources, and Young-Joo Lee for help with calculations. The authors wish to thank Toyoko Arai, Roland Bennowitz, and Werner Hofer for stimulating discussions and for critical comments on the manuscript.

<sup>1</sup>*Noncontact Atomic Force Microscopy*, edited by S. Morita, R. Wiesendanger, and E. Meyer, (Springer, Berlin, 2002).

<sup>2</sup>M. Bammerlin, R. Lüthi, E. Meyer, A. Baratoff, J. Lue, M. Guggisberg, C. Loppacher, C. Gerber, and H.J. Güntherodt, *Appl. Phys. A: Mater. Sci. Process.* **66**, S293 (1998).

<sup>3</sup>M. Reichling and C. Barth, *Phys. Rev. Lett.* **83**, 768 (1999).

<sup>4</sup>C. Barth, A.S. Foster, M. Reichling, and A.L. Shluger, *J. Phys.:*

*Condens. Matter* **13**, 2061 (2001).

<sup>5</sup>R. Bennowitz, S. Schär, V. Barwich, O. Pfeiffer, E. Meyer, F. Krok, B. Such, J. Kolodziej, and M. Szymanski, *Surf. Sci.* **474**, L197 (2001).

<sup>6</sup>K. Fukui, H. Onishi, and Y. Iwasawa, *Phys. Rev. Lett.* **79**, 4202 (1997).

<sup>7</sup>C.L. Pang, H. Raza, S.A. Haycock, and G. Thornton, *Appl. Surf.*

- Sci. **157**, 233 (2000).
- <sup>8</sup>A. Schwarz, W. Allers, U.D. Schwarz, and R. Wiesendanger, Phys. Rev. B **62**, 13 617 (2000).
- <sup>9</sup>M. Ashino, Y. Sugawara, S. Morita, and M. Ishikawa, Phys. Rev. Lett. **86**, 4334 (2001).
- <sup>10</sup>T. Kubo and H. Nozoye, Phys. Rev. Lett. **86**, 1801 (2001).
- <sup>11</sup>K. Fukui, Y. Namai, and Y. Iwasawa, Appl. Surf. Sci. **188**, 252 (2002).
- <sup>12</sup>W. Allers, A. Schwarz, U.D. Schwarz, and R. Wiesendanger, Europhys. Lett. **48**, 276 (1999).
- <sup>13</sup>K. Fukui, H. Onishi, and Y. Iwasawa, Chem. Phys. Lett. **280**, 296 (1997).
- <sup>14</sup>A. Sasahara, H. Uetsuka, and H. Onishi, J. Phys. Chem. B **105**, 1 (2001).
- <sup>15</sup>T. Fukuma, K. Kobayashi, K. Noda, K. Ishida, T. Horiuchi, H. Ymada, and K. Matsushige, Surf. Sci. **516**, 103 (2002).
- <sup>16</sup>A.I. Livshits, A.L. Shluger, A.L. Rohl, and A.S. Foster, Phys. Rev. B **59**, 2436 (1999).
- <sup>17</sup>A.S. Foster, C. Barth, A.L. Shluger, and M. Reichling, Phys. Rev. Lett. **86**, 2373 (2001).
- <sup>18</sup>R. Pérez, M. Payne, I. Stich, and K. Terakura, Phys. Rev. Lett. **78**, 678 (1997).
- <sup>19</sup>R. Pérez, I. Stich, M. Payne, and K. Terakura, Phys. Rev. B **58**, 10 835 (1998).
- <sup>20</sup>F.J. Giessibl, S. Hembacher, H. Bielefeldt, and J. Mannhart, Science **289**, 422 (2000).
- <sup>21</sup>S.H. Ke, T. Uda, and K. Terakura, Phys. Rev. B **65**, 125417 (2002).
- <sup>22</sup>M.A. Lantz, H.J. Hug, P.J.A. van Schendel, R. Hoffmann, S. Martin, A. Baratoff, A. Abdurixit, H.J. Güntherodt, and C. Gerber, Phys. Rev. Lett. **84**, 2642 (2000).
- <sup>23</sup>R. Bennewitz, A.S. Foster, L.N. Kantorovich, M. Bammerlin, C. Loppacher, S. Schär, M. Guggisberg, E. Meyer, and A.L. Shluger, Phys. Rev. B **62**, 2074 (2000).
- <sup>24</sup>A.L. Shluger, A.I. Livshits, A.S. Foster, and C.R.A. Catlow, J. Phys.: Condens. Matter **11**, R295 (1999).
- <sup>25</sup>J. Tóbiik, I. Stich, R. Pérez, and K. Terakura, Phys. Rev. B **60**, 11 639 (1999).
- <sup>26</sup>S.H. Ke, T. Uda, R. Pérez, I. Stich, and K. Terakura, Phys. Rev. B **60**, 11 631 (1999).
- <sup>27</sup>A.I. Livshits and A.L. Shluger, Faraday Discuss. **106**, 425 (1997).
- <sup>28</sup>T.R. Albrecht, P. Grütter, D. Horne, and D. Rugar, J. Appl. Phys. **69**, 668 (1991).
- <sup>29</sup>P.V. Sushko, A.S. Foster, L.N. Kantorovich, and A.L. Shluger, Appl. Surf. Sci. **144-145**, 608 (1999).
- <sup>30</sup>A.S. Foster, A.L. Shluger, and R.M. Nieminen, Appl. Surf. Sci. **188**, 306 (2002).
- <sup>31</sup>D.H. Gay and A.L. Rohl, J. Chem. Soc., Faraday Trans. **91**, 925 (1995).
- <sup>32</sup>M. Guggisberg, M. Bammerlin, C. Loppacher, O. Pfeiffer, A. Abdurixit, V. Barwich, R. Bennewitz, A. Baratoff, E. Meyer, and H.-J. Güntherodt, Phys. Rev. B **61**, 11 151 (2000).
- <sup>33</sup>A.S. Foster, L.N. Kantorovich, and A.L. Shluger, Appl. Phys. A: Mater. Sci. Process. **72**, S59 (2000).
- <sup>34</sup>R.H. French, R.M. Cannon, L.K. DeNoyer, and Y.M. Chiang, Solid State Ionics **75**, 13 (1995).
- <sup>35</sup>J. Junquera, O. Paz, D. Sánchez-Portal, and E. Artacho, Phys. Rev. B **65**, 235111 (2001).
- <sup>36</sup>J.M. Soler, E. Artacho, J.D. Gale, A. García, J. Junquera, P. Ordejón, and D. Sánchez-Portal, J. Phys.: Condens. Matter **14**, 2745 (2002).
- <sup>37</sup>J.P. Perdew, K. Burke, and M. Ernzerhof, Phys. Rev. Lett. **77**, 3865 (1996).
- <sup>38</sup>A.I. Livshits, A.L. Shluger, and A.L. Rohl, Appl. Surf. Sci. **140**, 327 (1999).
- <sup>39</sup>M.A. Lantz, H.J. Hug, R. Hoffman, P.J.A. van Schendel, P. Kappenberger, S. Martin, A. Baratoff, and H.J. Güntherodt, Science **291**, 2580 (2001).
- <sup>40</sup>R.S. Mulliken, J. Chem. Phys. **49**, 497 (1949).
- <sup>41</sup>A.L. Shluger, L.N. Kantorovich, A.I. Livshits, and M.J. Gillan, Phys. Rev. B **56**, 15 332 (1997).
- <sup>42</sup>M. Shimizu, H. Watanabe, K. Anazawa, T. Miyahara, and C. Manabe, J. Chem. Phys. **110**, 12 116 (1999).